Visualizing sporadic meteor radiants and their dynamics by radio forward scattering

Wolfgang Kaufmann[1]

Frequency gradients of forward scattered head echoes are used to distinguish between different sources of sporadic meteors. This approach requires a basic radio station only. By means of kernel density mapping the antihelion, apex and helion source could be displayed as well as their dynamic composition of different radiants in time and space during a continuous 40 day measuring campaign. The study of the dynamics was performed with a 10 day as well as a daily resolution.

Received 2018 September 5

1 Introduction

Sporadic meteors are considered as meteors not being part of a recognized shower. The distribution of the radiants of sporadic meteors within the celestial sphere were subject of a number of surveys. Since 1959 it is known that the sources of sporadic meteors are non-homogeneously distributed in space (Hawkins, 1956). Jones and Brown (1993) identified 6 regions with increased activity: north and south toroidal source, antihelion (AH) and helion (H) source and north and south apex (AP). Seasonal variations also were studied and revealed the dynamics of the single sources throughout the year (Campell-Brown & Jones, 2006; Campell-Brown & Wiegert, 2009). The effect of the visibility of the sources in dependence of latitude and season of year on the observed meteor count rates was investigated by Younger et al. (2009).

For the meteor amateur astronomer as an individual such studies are not easily to accomplish. An optical observation delivers concrete directional parameters of observed meteors but is restricted to night time and clear skies. A basic meteor radio station in standard mode provides no directional information but can be used for observation 24 hours a day. This paper describes a qualitative approach to study the dynamics of sporadic meteor occurrence based on radio forward scatter. Only prerequisite is a radio meteor receiving and detecting system that is able to pick up the frequency change of meteor head echoes with a sufficient time and frequency resolution.

Utilising meteor head echoes can provide directional information. The frequency of radio waves scattered at the plasma sheet surrounding the meteoroid during its flight through the terrestrial atmosphere (Close et al., 2002) is continuously altering. This is a result of the changing radial velocities of the meteoroid with respect to the observer and to the transmitter, as well as its deceleration during its flight. Different radial velocity changes generate different frequency gradients as long as the scattering originates from a circumscribed fixed region. They attribute to meteoroids of different origin in terms of altitude, azimuth and geocentric velocity. Because the meteoroid-receiver geometry is unknown a concrete position in the celestial sphere cannot be calculated from the frequency gradients. However a statistical method, the Kernel Density Map (KDM), can make visible the distribution of the frequency gradients of meteor head echoes thereby indicating different radiants (Kaufmann, 2018). The closer and more numerous the frequency gradients cluster at different positions in a frequency gradient vs. time diagram the higher the calculated local density (via a kernel function) will be. This local density is displayed by a shade of grey in the KDM. Thus a hot spot means there is a bunch of meteors having very similar frequency slopes at a certain time. This basically can be ascribed to a common origin in space, i.e. this bunch of meteors is an indication for a (micro)shower.

By this technique the dynamics of emerging and disappearing of micro showers and the fluctuation of activity within the broad persistent sporadic meteor sources can be studied at least qualitatively. The results of a measuring campaign from January to February 2018 are presented.

2 Material and Methods

The French radar-transmitter GRAVES was employed for forward scattering. It transmits a continuous rf-signal at a frequency of 143.050 MHz and illuminates a well defined region of the sky in 100 km height over southern France. Receiving location was Algermissen, Northern Germany (N 52°15′.16, E 009°58′.71). A HB9CV antenna was directed to the transmitter location and fed to a FUNcube Dongle Pro+ (FCDP). The FCDP is a software defined receiver[a]. This means all filtering and demodulation is done by software. SDR# was used as receiving software[b]. It was set to USB, 143.049 MHz receiving frequency, 48 kHz audio output, audio filtering and AGC switched off. The audio output was fed to the software Meteor Logger[c], which detects and logs meteor signals within an audio stream (Kaufmann, 2017). It reveals a continuous output i.a. of the frequency of the detected signal in 10.7 ms steps. Both programs ran on the same computer (Intel i5, clock speed 2.3 GHz) with Windows 7. Observation period was 2018 January 5 to February 17.

The software Process Data[c] was used to edit the gathered raw data. It filtered out interference, merged intermitted meteor signals, identified the head echoes

[1]Lindenweg 1e, 31191 Algermissen, Germany.
Email: contact@ars-electromagnetica.de

IMO bibcode WGN-466-kaufmann-vizualizing
NASA-ADS bibcode 2018JIMO...46..201K

[a]http://www.funcubedongle.com/
[b]https://airspy.com/download/
[c]http://www.ars-electromagnetica.de/robs/download.html

Table 1 – Main issues of the observation period 2018 January 5, 17^h UTC to February 17, 16^h59^m UTC.

Observing Time [h]	Total Counts	Head Echo Counts	% Head Echoes	Mean Head Echoes/h
1030	34280	3443	10.04 %	3.3

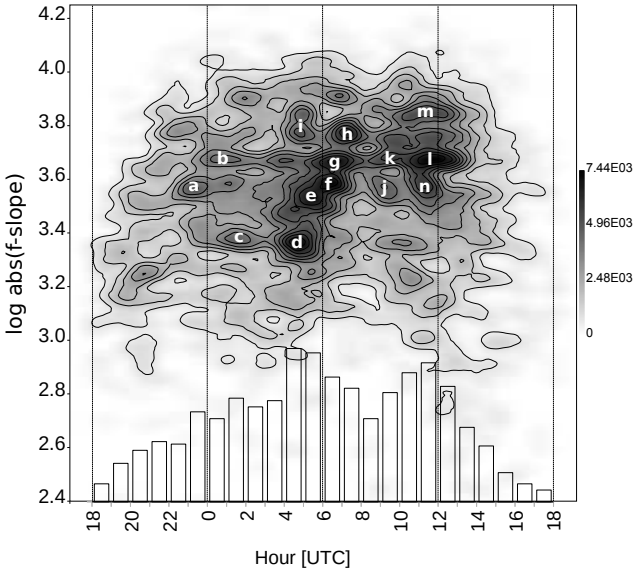

Figure 1 – Kernel density map of the frequency slopes of head echoes from 40 × 24 h of continuous observation (Jan 5 – Feb 14). The cumulated head echo counts per hour are added as bar chart (Maximum 247 Head echoes/h). Daily time span is $18^h - 17^h59^m$ UTC. The positions of high density hotspots are marked by lower cases.

and calculated its frequency gradients. The decadic logarithm of the absolute value of the frequency gradients was calculated and plotted as a KDM by means of the statistical software PAST[d]. In detail this procedure is described in Kaufmann (2018).

3 Results

The observation was started at the beginning of 2018 shortly after the Quadrantids maximum. It was extended to mid-February. This time span was free of major meteor showers which allowed for an unbiased observation of the sporadic meteors. Table 1 outlines the result. The low number of head echoes is caused by the low radar cross section (RCS) of the plasma sheet, surrounding the travelling meteoroid. E.g. Close et al. (2002) found a maximum RCS of 0.14 m^2 at 160 MHz for the Leonids. So only head echoes from meteoroids of higher masses are captured.

A bar plot of the totalled hourly head echo counts of 40 days of observation is shown in Figure 1. Three peaks can be detected between $23^h - 02^h$, $04^h - 07^h$ and $10^h - 13^h$ UTC, respectively. To uncover continuous sources of sporadic meteors all frequency gradients of head echoes of the 40 day observation period were combined in one KDM, see Figure 1. For an insight in the sporadic meteor dynamics 4 consecutive KDM were created each comprising 10 days of observation, see Figure 2A–D. Each KDM displays the distribution of the measured frequency gradients in the time span $18^h - 17^h59^m$ UTC (local time CET = UTC + 1). Hot spots in a KDM mark a high number of similar frequency gradients.

At least to get an idea of the daily dynamics of sporadic meteors a ternary plot was created. For this purpose three timeframes were adopted and centred around the noticed three peaks of the hourly head echo counts (Figure 1). Each timeframe comprised three hours of observation: $23^h - 02^h$, $04^h - 07^h$ and $10^h - 13^h$ UTC. All observed head echoes being within these three timeframes were counted per day and depicted as daily proportion, see Figure 3. The number of head echoes within a timeframe is rather small (2–30). So random fluctuation within each timeframe will have a noticeable impact on their numeric proportions and must be taken in account.

4 Discussion

The bar plot of the hourly count rates of the head echoes (see Figure 1) exhibits three peaks. They occur at daytimes that coincide with the highest radiant positions in the sky of the AH, AP and H source, respectively (Lunsford, 2009). The proportion of these three peaks agrees with the measured activities of the AH, AP and H source by Campbell-Brown and Jones (2006). It can be assumed that these peaks are mainly the manifestation of the activity of the AH, AP and H source with minor contribution of the northern toroidal source as well as sporadic meteors that do not belong to one of these sources. Referring to the IMO 2018 working list (Rendtel, 2017) the GUM, DCS and DXC may be considered also.

The rising and falling of radiant positions due to Earth's rotation do not depict as tracks in the KDMs (Figure 1 and 2). This is due to the restricted sensitivity of the receiving system: only at a high altitude of the radiant the number of detectable head echoes is high enough to constitute noticeable densities becoming visible as hot spot in the KDM. Figure 1 and 2 are composed from several days of observation. So higher densities can result from persistent radiants of lower activity or short term radiants of higher activity.

The different hot spots emerge from clusters of common frequency slopes of the head echoes and indicate different radiant positions and/or geocentric velocities. In Figure 1 the hot spots exhibiting higher density are marked with lowercases a–n. They can be clustered into three groups by daytime which can be assigned to the AH (a–c), the AP (d–i) and to the H (j–n) peak of the head echo count rates. So for the period 2018 January 05 – February 14 at least 14 different major radiants could be distinguished basically within the AH, AP and H source by this technique. However there are more hot spots albeit of lesser density spread over the KDM. As

[d] http://folk.uio.no/ohammer/past/

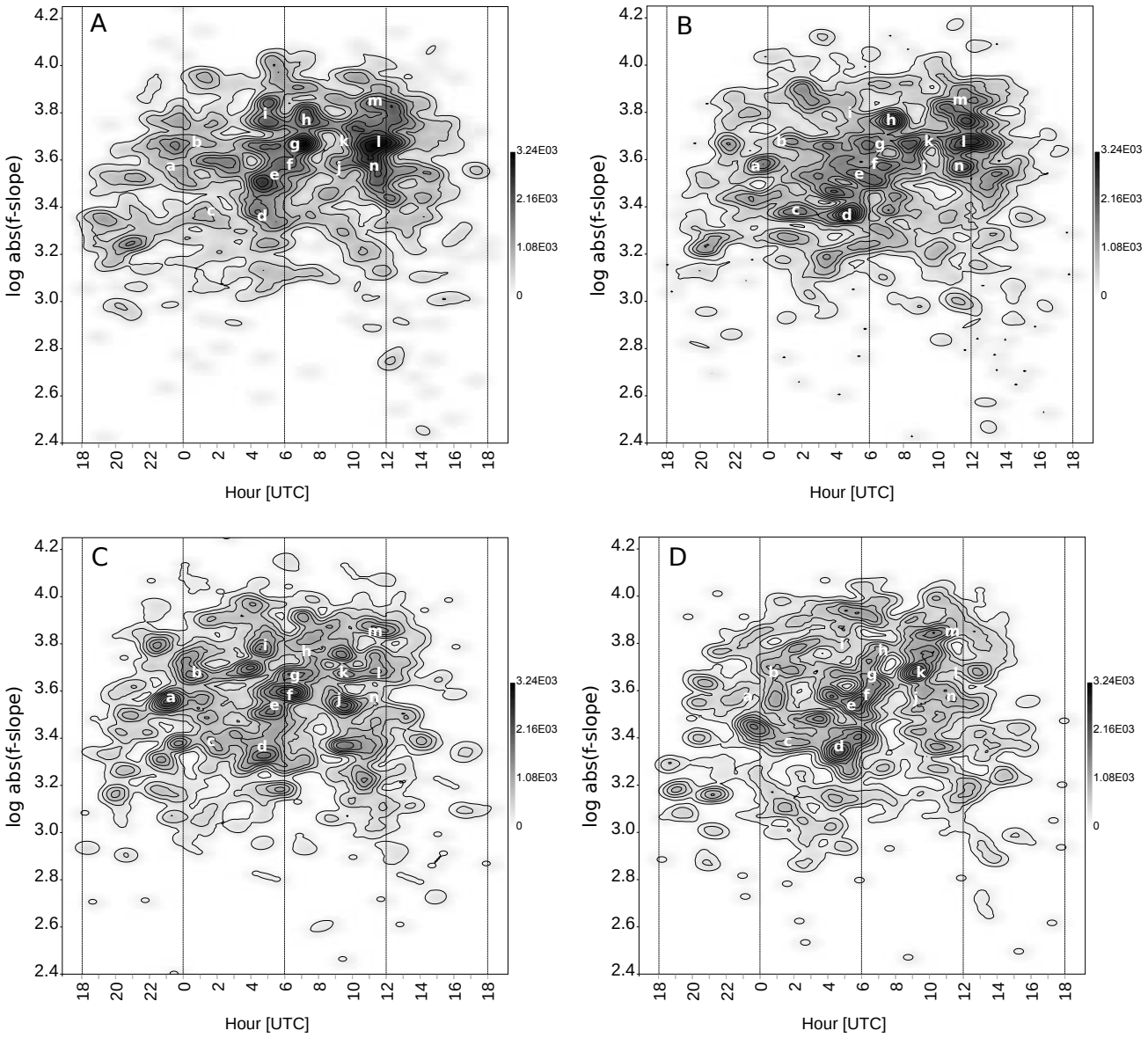

Figure 2 – Kernel density maps of the frequency slopes of head echoes each from 10×24 h of continuous observation: A) Jan 5 – Jan 15, B) Jan 15 – Jan 25, C) Jan 25 – Feb 04 and D) Feb 04 – Feb 14). Daily time span is $18^{\mathrm{h}} - 17^{\mathrm{h}}59^{\mathrm{m}}$ UTC. The positions marked by lower cases are copied from Figure 1.

weak showers they may be also part of the AH, AP and H source if occurring at the peak times of the head echo count rates.

Figures 2A to 2D give information about the persistence of the radiants of Figure 1. A comparison of the appearance of the marked radiants within the four intervals of the observation period (OBP) yields different trends, e.g.:

- a, b and c are most active in the middle of the OBP (2B, 2C),
- h is most active in the beginning of the OBP (2A, 2B),
- k is most active at the end of the OBP (2C, 2D),
- d is present over the complete OBP with a fluctuating activity,
- l is present over the complete OBP with a declining activity.

The major radiants of the AH, AP and H source obviously appear only for a limited period of time. So the AH, AP and H sources are composed of radiants not only differing in spatial position but also in time of activity.

Due to decreased averaging time in Figure 2 more weak short term radiants emerge. They are present only in one of the individual KDMs and are spread over the whole daytime and frequency gradient span. All in all the "continuous sporadic background" obviously is a result of a complex and highly irregular interplay of sporadic meteors in space and time. Belkovich (1995) stated that the radiant distribution is rather similar for the same time intervals in different years.

At least for an investigation of the daily dynamics of sporadic meteors the proportions of three specific daily count rates of head echoes are compiled in a ternary plot, see Figure 3. The specified portions of counts can be assigned mainly to the AH ($23^{\mathrm{h}}-02^{\mathrm{h}}$), AP ($04^{\mathrm{h}}-07^{\mathrm{h}}$)

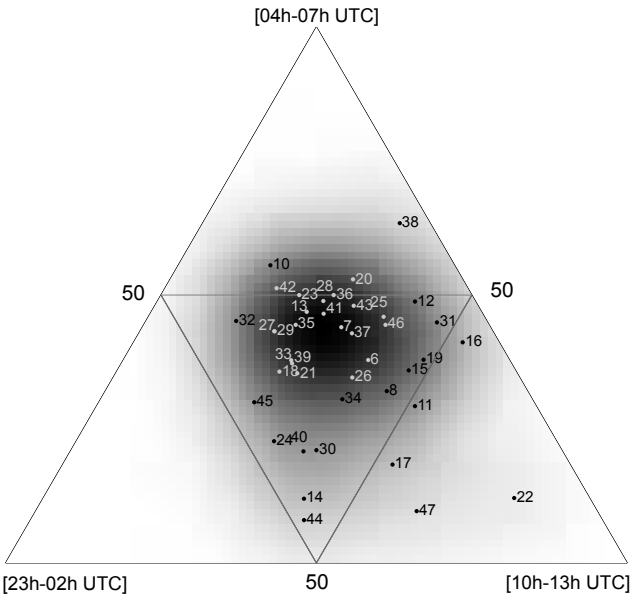

Figure 3 – Ternary plot of the daily proportions of the number of head echoes counted within each of the indicated timeframes (see also text). The dots were indexed by their calendar day (6–47 = Jan 6 – Feb 16). The point density is calculated by means of a kernel density method by the statistical software PAST.

and H ($10^{\mathrm{h}} - 13^{\mathrm{h}}$) source. A great variety of different proportions is shown. Ignoring the outliers as a result of the small numbers of counts no proportion seem to be preferred. The proportions are spread onto an area of circle as indicated by a circular point density distribution. The position of the centroid of the density distribution is determined by the mean proportion of the AH, AP and H activity. Furthermore the shape of the density distribution suggests a multivariate normal distribution of the combinations of activities of the AH, AP and H source. Hence consecutive calendar days do not show a trend in their proportions, the series of proportions is highly irregular.

This situation is the crux of numerical observations by radio forward scatter with a basic system: there is no procedure to precisely distinguish between the contribution of sporadic meteors and the shower under investigation. A widely used technique is to calculate a mean diurnal sporadic activity per hour from pre-recorded data that can be subtracted from the observed total number of counts per hour. The irregularity of the sporadic background nevertheless will imprint on the result. So smaller variations in the resulting counts per hour must not be interpreted unverified as changes in meteor flux or meteor mass distribution of the observed shower.

5 Conclusion

The technique of using frequency gradients of forward scattered head echoes to gain additional positional information demonstrated to be useful to:

- observe the concentration of sporadic meteors in the AH, AP and H source,
- differentiate major radiants in the AH, AP and H source (within the observing period 14 major radiants could be distinguished), and
- visualise the dynamics of the radiants within AH, AP and H sources as well as the dynamic occurrence of random weak and micro showers beyond these sources resulting in a continuous sporadic background.

The numerical analysis of the ratio of the activity of the AH, AP and H source on a daily base showed its high variability and unpredictability. Therefore using pre-recorded sporadic meteor counts for correction of subsequent shower records may be handled with care.

References

Belkovich O. I., Filimonova T. K., and Sidorov V. V. (1995). "Structure of sporadic meteor radiant distributions from radar observations". *Earth, Moon, and Planets*, **68**, 199–205.

Campell-Brown M. D. and Jones J. (2006). "Annual variation of sporadic radar meteor rates". *Mon. Not. R. Astron. Soc.*, **367:2**, 709–716.

Campell-Brown M. D. and Wiegert P. (2009). "Seasonal variations in the north toroidal sporadic meteor source". *Meteoritics and Planetary Science*, **44:12**, 1837–1848.

Close S., Oppenheim M., Hunt S., and Dryud L. (2002). "Scattering characteristics of high-resolution meteor head echoes detected at multiple frequencies". *J. Geophs. Res.*, **107:A10**. SIA 9 (1-12).

Hawkins G. S. (1956). "A radio echo survey of sporadic meteor radiants". *Mon. Not. R. Astron. Soc.*, **116**, 92–104.

Jones J. and Brown P. (1993). "Sporadic meteor radiant distribution: orbital survey results". *Mon. Not. R. Astron. Soc.*, **265**, 524–532.

Kaufmann W. (2017). "New radio meteor detecting and logging software". *WGN, Journal of the IMO*, **45:4**, 67–72.

Kaufmann W. (2018). "Visualizing meteor streams by radio forward scattering on the basis of meteor head echoes". *WGN, Journal of the IMO*, **46:1**, 39–44.

Lunsford R. (2009). *Meteors and How to Observe Them.* Springer, New York.

Rendtel J. (2017). "2018 Meteor Shower Calendar". International Meteor Organization, Potsdam. IMO_INFO (2-17).

Younger P. T., Astin I., Sandford D. J., and Mitchell N. J. (2009). "The sporadic radiant and distribution of meteors in the atmosphere as observed by VHF radar at Arctic, Antarctic and equatorial latitudes". *Ann. Geophys.*, **27**, 2831–2841.

Handling Editor: Jean-Louis Rault